An Optimization-Based Discontinuous Galerkin Approach for High-Order Accurate Shock Tracking with Guaranteed Mesh Quality

Andrew Shi*
Department of Mathematics, University of California, Berkeley, Berkeley, CA 94720, U.S.A.

Per-Olof Persson†
Department of Mathematics, University of California, Berkeley, Berkeley, CA 94720, U.S.A.

Matthew J. Zahr‡
Department of Aerospace and Mechanical Engineering, University of Notre Dame, Notre Dame, IN 46556, U.S.A.

High-order accurate discontinuous Galerkin (DG) methods have recently become popular for the simulation of a wide range of flow problems. However, for shocks and other discontinuities, these methods have to be stabilized by techniques such as limiting or artificial viscosity, leading to a first-order accurate method that requires very aggressive mesh adaptivity and a large number of elements. This work uses an alternative tracking-based technique for accurate solutions of these problems. Inspired by the fact that the DG method allows for discontinuities between all the mesh elements, we formulate a so-called r-adaptive method which moves the mesh in order to align the mesh edges with the jumps in the solution. This has the potential to obtain high-order accuracy with drastically fewer elements and lower computational cost. The proposed tracking method is based on a PDE-constrained optimization formulation, where the representation of the curved high-order mesh is used as optimization variables, the high-order DG discretization is enforced as a constraint, and the objective function is a discontinuity indicator with properties that make it well-suited for a gradient-based optimizer. A full space solver is used to converge the mesh and the solution simultaneously and it does not require solving the discrete PDE on intermediate non-aligned meshes. In previous work, the objective function also included a penalty term to regularize the element qualities and prevent inversion. This introduces a problem-dependent parameter which is difficult to determine, and it also leads to a compromise between the tracking objective and the element qualities. In this work, the mesh qualities are instead controlled by nonlinear constraints, and the shock tracking objective function is minimized among a large class of deformed meshes that satisfy a given quality condition. The mesh quality parameter in this formulation is easier to prescribe and it is essentially problem independent. Furthermore, it allows for a more precise minimization of the tracking objective function and potentially more accurate solutions. The method is demonstrated on Burgers' equation in 1D and supersonic flow around a cylinder in 2D.

I. Introduction

While it is clear that the discontinuous Galerkin (DG) and related high-order methods [1–3] are getting sufficiently mature to handle realistic problems in aerodynamics, they are still suffering from the lack of nonlinear stability. This limits their impact on many important applications, in particular ones involving shocks since even small oscillations in the solution can cause non-physical results.

Several approaches have been proposed for handling shocks. One simple method is to use a sensor that identifies the elements in the shock region and reduces the order of interpolating polynomials [4, 5]. This is usually combined with

*Department of Mathematics, University of California, Berkeley, Berkeley CA 94720-3840. Email: andrewshi94@berkeley.edu. AIAA Student Member.

†Associate Professor, Department of Mathematics, University of California, Berkeley, Berkeley CA 94720-3840. Email: persson@berkeley.edu. AIAA Senior Member.

‡Assistant Professor, Department of Aerospace and Mechanical Engineering, University of Notre Dame, Notre Dame, IN 46556-5637. Email: mzahr@nd.edu. AIAA Member.

h-adaptivity to better resolve the shocks, and it can be quite satisfactory for in particular steady-state problems. More sophisticated approaches include limiting, for example based on weighted essentially non-oscillatory (WENO) concepts [1, 6]. Another popular approach is the artificial viscosity technique for subcell shock capturing presented in Ref. [7] and [8]. Inspired by the early artificial viscosity methods [9], this approach has proven to be surprisingly effective in the context of high-order DG methods. The method combines a highly selective spectral sensor with a consistently discretized artificial viscosity added to the equations. This smoothing of the discontinuities gives a number of important benefits, such as fully converged steady-state solutions and smooth behavior of moving shocks.

However, shock capturing techniques such as limiting and artificial viscosity all have the drawback that the accuracy is reduced to first order in the affected elements, which leads to a formal first order global accuracy. While this can be partially offset with appropriate h-adaptivity, in particular using anisotropic elements around the shock, it does pose a major limitation and makes it unclear if high-order methods can be competitive for these applications.

Recently, we introduced an alternative approach for handling shocks in a high-order DG method [10], which is more closely related to shock tracking and r-refinement than shock capturing. It is based on the observations that if a (curved) face of an element is perfectly aligned with a shock, the approximate Riemann solver will provide the appropriate stabilization and allow for high-order approximations of the solution on both sides of the discontinuity. The difficulty with these methods is that the DG method without additional stabilization is highly sensitive to the location of the elements, and a very small mismatch will in general result in oscillations and prevent convergence. Instead we recast the nonlinear, discrete equations as a PDE-constrained optimization problem where the objective function is an appropriate shock indicator, the constraints are the DG discretization of the conservation law, and the optimization variables are the discrete PDE solution and the positions of the nodes of the mesh. The mesh deformation is handled by transforming the conservation law to a fixed reference domain through a diffeomorphism. This means the mesh nodes will be aligned in a consistent way with the current numerical solution (and not, e.g., the true physical position), but also that we can obtain converged solutions using efficient constrained optimization methods.

In our previous work, the optimization objective function also included a penalty term to control the mesh qualities and prevent inversion. While this generated good results, it introduced a problem-dependent parameter and led to compromises in the minimization of the tracking indicator. In this paper, we present an alternative technique which instead enforces the mesh qualities through nonlinear constraints. This allows for minimization of the tracking objective function among a large class of deformed meshes where the elements satisfy a given quality constraint. This parameter is more natural to prescribe and should be highly problem independent. We also expect this formulation to produce more accurate mesh alignment with the solution discontinuities.

We review all the components of our framework, and in particular emphasize the details of our new formulation and how the mesh quality constraints are incorporated. We demonstrate the method on Burgers' equation in 1D and on the Euler equations of gas dynamics in 2D for a supersonic flow problem around a cylinder.

II. Governing equations and spatial discretization

Consider a general system of N_c steady, inviscid conservation laws, defined on the physical domain $\Omega \subset \mathbb{R}^d$,

$$\nabla \cdot \mathcal{F}(U) = 0 \quad \text{in } \Omega, \tag{1}$$

where $U(x) \in \mathbb{R}^{N_c}$ is the solution of the system of conservation laws at $x \in \Omega \subset \mathbb{R}^d$ and $\mathcal{F}(U) \in \mathbb{R}^{N_c \times d}$ is the physical flux. We assume that the solution U contains discontinuities, such as shock waves, in which case the conservation law (1) holds away from these discontinuities.

A. Transformed conservation law on fixed reference domain

Following our previous work [10] where we use deformation of the computational mesh, and therefore the physical domain, to track discontinuities, we reformulate the conservation law on a fixed reference domain, Ω_0. Let $\mathcal{G} : \mathbb{R}^d \times \mathbb{R}^{N_\mu} \to \mathbb{R}^d$ be a parametrized diffeomorphism defining the map from reference to physical domain (Figure 1), i.e.,

$$\Omega = \mathcal{G}(\Omega_0, \mu), \tag{2}$$

where $\mu \in \mathbb{R}^{N_\mu}$ is a vector of parameters. Under the domain mapping (2), the conservation law becomes

$$\nabla \cdot \mathcal{F}(U) = 0 \quad \text{in } \mathcal{G}(\Omega_0, \mu). \tag{3}$$

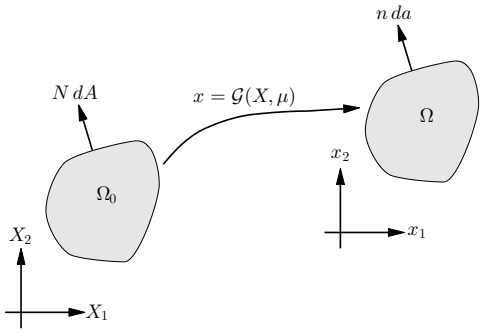

Fig. 1 Mapping between reference and physical domains.

The conservation law on the physical domain Ω is transformed to a conservation law on the reference domain Ω_0 using the procedure in [11] to yield

$$\nabla_X \cdot F(u,\ \mu) = 0 \quad \text{in } \Omega_0 \tag{4}$$

where ∇_X denotes spatial derivatives with respect to the reference domain Ω_0 with coordinates X. The transformed state vector, u, and flux, F, take the form

$$u = g_\mu U, \qquad F(u,\ \mu) = g_\mu \mathcal{F}(g_\mu^{-1} u) G_\mu^{-T} \tag{5}$$

where $G_\mu(X) = \frac{\partial}{\partial X}\mathcal{G}(X,\ \mu)$ is the deformation gradient of the domain mapping and $g_\mu(X) = \det G_\mu(X)$ is the Jacobian. For details regarding the derivation of the transformed equations, the reader is referred to [11].

B. Discontinuous Galerkin discretization of transformed conservation law

A standard nodal discontinuous Galerkin method is used to discretize the conservation law (1). Let $\mathcal{E}_{h,p}$ represent a discretization of the domain Ω_0 into non-overlapping, potentially curved, computational elements, where h is a mesh element size parameter and p is the polynomial order associated with the curved elements. The discontinuous Galerkin formulation takes the form

$$\sum_{K \in \mathcal{E}_{h,p}} \int_{\partial K} \psi \cdot F^*(u,\ \mu,\ N)\, dA - \int_{\Omega_0} F(u,\ \mu) : \nabla_X \psi\, dV = 0, \tag{6}$$

where N is the outward normal to the surface ∂K and F^* is the numerical flux that ensures the flux is single-valued along ∂K where u is multi-valued.

To establish the finite-dimensional form of (6), we introduce the isoparametric finite element space of piecewise polynomial functions associated with the mesh $\mathcal{E}_{h,p}$:

$$\mathcal{V}_{h,p} = \left\{ v \in [L^2(\Omega_0)]^{N_c} \mid v|_K \circ \mathcal{T}_K \in [\mathcal{P}(K_0)]^{N_c}\ \forall K \in \mathcal{E}_{h,p} \right\}$$

where $\mathcal{P}_p(K_0)$ is the space of polynomial functions of degree at most $p \geqslant 1$ on the parent element K_0 and $K = \mathcal{T}_K(K_0)$ defines a mapping from the parent element to element $K \in \mathcal{E}_{h,p}$. For notational brevity, we assume all elements map from a single parent element. Then the Galerkin weak form in (6) becomes: find $u_{h,p} \in \mathcal{V}_{h,p}$ such that for all $\psi_{h,p} \in \mathcal{V}_{h,p}$

$$\sum_{K \in \mathcal{E}_{h,p}} \int_{\partial K} \psi_{h,p} \cdot F^*(u_{h,p},\ \mu,\ N)\, dA - \int_{\Omega_0} F(u_{h,p},\ \mu) : \nabla_X \psi_{h,p}\, dV = 0. \tag{7}$$

Finally, we introduce a basis $\{\varphi_i\}_{i=1}^{N_p}$ for $\mathcal{P}_p(K_0)$ to obtain the discrete form of (7)

$$\boldsymbol{r}(\boldsymbol{u},\ \boldsymbol{x}) = 0, \tag{8}$$

where $\boldsymbol{u} \in \mathbb{R}^{N_{\boldsymbol{u}}}$ is the vector of solution coefficients for all elements and $\boldsymbol{x} \in \mathbb{R}^{N_{\boldsymbol{x}}}$ are the nodal positions of the *continuous, high-order mesh* to ensure nodes co-located in the reference domain will be co-located in the physical domain. With this notation, the continuous domain mapping is parametrized by $\mu = \boldsymbol{x}$, i.e., $\Omega = \mathcal{G}(\Omega_0,\ \boldsymbol{x})$. The remainder of the document will use $\boldsymbol{x}$ to parametrize the domain deformation instead of μ.

III. High-order shock tracking via constrained optimization

In this section, we present an optimization framework designed to align discontinuous features in a finite-dimensional solution basis with features in the solution itself. In the discretization setting outlined in Section II, this amounts to aligning element faces, where discontinuities are supported, with discontinuities in the solution. With the discontinuous features tracked with element faces, very coarse high-order discretizations are effectively used to resolve the smooth solution throughout the domain. To align element faces with solution discontinuities, a constrained optimization formulation of the DG equations is employed that simultaneously seeks the DG solution, $\boldsymbol{u}$, and the nodal positions of the continuous (high-order) mesh, $\boldsymbol{x}$, that minimizes an appropriate objective function and satisfies the discrete DG equations (8). In addition, *constraints* on the distortion of the elements in the mesh are included to ensure the mesh remains well-conditioned. Our previous work [10] included a penalization term on the mesh distortion in the objective function, which led to a penalty parameter that was difficult to interpret and select. That is, small penalty parameters are needed to ensure the shock is appropriately tracked, while moderate values are needed to keep the mesh well-conditioned. Non-zero values of the penalty parameter inevitably leads to a trade-off between precision to which discontinuities are tracked and quality of the mesh. Including the mesh distortion as a constraint ensures the objective function is solely dedicated to shock tracking among the set of meshes that satisfy the distortion constraints.

A. Shock tracking optimization formulation with mesh distortion constraints

The goal of the tracking framework is to align faces of the DG mesh with the discontinuity. Since the discontinuity is not known *a-priori*, a mesh cannot be constructed to explicitly conform to the shock. Instead, we consider a parametrization of the nodal positions of the continuous, high-order mesh $\boldsymbol{x} = \boldsymbol{x}(\boldsymbol{\phi}) = \mathcal{A}(\boldsymbol{\phi})$, where $\boldsymbol{\phi} \in \mathbb{R}^{N_{\boldsymbol{\phi}}}$ is a vector of parameters. In the most general case, each degree of freedom of node of the mesh is an optimization parameter and $\mathcal{A}(\boldsymbol{\phi}) = \boldsymbol{\phi}$ is the identity map; however, the mapping $\mathcal{A}(\boldsymbol{\phi})$ can be used to build any *a-priori* knowledge of the shock location into the parametrization or steps that ensure the resulting mesh is well-conditioned, e.g., smoothing.

With this parametrization, the problem of solving the discrete PDE on a fixed mesh, i.e., $\boldsymbol{r}(\boldsymbol{u}, \boldsymbol{x}) = 0$ where $\boldsymbol{x}$ is given, is replaced with the optimization problem

$$\begin{aligned} \underset{\boldsymbol{u},\boldsymbol{\phi}}{\text{minimize}} \quad & f_{shk}(\boldsymbol{u}, \boldsymbol{x}(\boldsymbol{\phi})) \\ \text{subject to} \quad & f^K_{msh}(\boldsymbol{x}(\boldsymbol{\phi})) \leqslant \bar{f}_{msh}, \quad K \in \mathcal{E}_{h,p} \\ & \boldsymbol{r}(\boldsymbol{u}, \boldsymbol{x}(\boldsymbol{\phi})) = 0, \end{aligned} \tag{9}$$

where $f_{shk}(\boldsymbol{u}, \boldsymbol{x})$ is a shock-indicating objective function and $f^K_{msh}(\boldsymbol{x})$ is the distortion of element $K \in \mathcal{E}_{h,p}$. This optimization problem seeks to find the mesh $\boldsymbol{x}(\boldsymbol{\phi})$ and solution $\boldsymbol{u}$ that minimize $f_{shk}(\boldsymbol{u}, \boldsymbol{x})$ while satisfying the discretized PDE and mesh quality constraints.

B. Shock tracking objective function

An effective objective function for the optimization formulation in (9) must monotonically approach a (local) minimum in the feasible set as $\boldsymbol{x} \to \boldsymbol{x}^*$, where $\boldsymbol{x}^*$ is any mesh that aligns with the shock. While residual-based error indicators are popular in the mesh adaptation community, we have observed that these fail to *monotonically* approach a local minima. The indicator used in this work is the integrated deviation of the solution from the mean in each element:

$$f_{shk}(\boldsymbol{u}, \boldsymbol{x}) = \sum_{K \in \mathcal{E}_{h,p}} \int_{\mathcal{G}(K,\boldsymbol{x})} \left\| u_{h,p} - \bar{u}^K_{h,p} \right\|^2_{\boldsymbol{W}} \, dV \tag{10}$$

where the dependence of the finite dimensional solution $u_{h,p}$ on the discrete representation is implied, $\bar{u}^K_{h,p}$ is the mean value of $u_{h,p}$ over element K, and $\boldsymbol{W} \in \mathbb{R}^{N_c \times N_c}$ is the symmetric positive semi-definite matrix that defines the local semi-norm,

$$\bar{u}^K_{h,p} = \frac{1}{|\mathcal{G}(K, \boldsymbol{x})|} \int_{\mathcal{G}(K,\boldsymbol{x})} u_{h,p} \, dV, \qquad |\mathcal{G}(K, \boldsymbol{x})| = \int_{\mathcal{G}(K,\boldsymbol{x})} dV. \tag{11}$$

In this work, we only consider $\boldsymbol{W} = \boldsymbol{e}_1^T \boldsymbol{e}_1$ (density component). While this objective does not provably satisfy the required objective function conditions, it seems to satisfy them in practice; see [10] for additional detail.

C. Mesh quality constraints

The discontinuity indicator in (10) is not well-suited as the objective function in the discontinuity-tracking optimization setting (9) in its current form because it is agnostic to a poor quality or inverted mesh that may arise from certain choices of $\boldsymbol{x}$. To avoid the mesh distortion that would result from solely minimizing f_{shk}, we include constraints on the elementwise mesh distortion in (9). Here, we define the mesh distortion as the deviation from the uniform element in one dimension and utilize a common mesh distortion metric in high-order mesh generation [12, 13] in higher dimensions

$$f_{msh}^{K}(\boldsymbol{x}) = \begin{cases} \left| \dfrac{h_0}{|\mathcal{G}(K,\, \boldsymbol{x})|} - 1 \right| & d = 1 \\ \dfrac{1}{|\mathcal{G}(K,\, \boldsymbol{x})|} \displaystyle\int_{\mathcal{G}(K,\, \boldsymbol{x})} \left(\dfrac{\|G_{h,p}\|_F^2}{\left(\det G_{h,p}\right)_+^{2/d}} \right)^r & \text{otherwise,} \end{cases} \tag{12}$$

for $K \in \mathcal{E}_{h,p}$, where $r = 2$ is used in this work and $G_{h,p} = \dfrac{\partial x_{h,p}}{\partial X}$ is the finite-dimensional deformation gradient.

D. Full space optimization solver

The optimization problem in (9) is solved using a full space approach that treats $\boldsymbol{u}$ and $\boldsymbol{\phi}$ as independent optimization variables and converges them simultaneously to their optimal values. This implies the solution of the PDE is *never required away from a discontinuity-aligned mesh* $\boldsymbol{x}^*$ and overcomes potential stability issues that would arise in a reduced space approach that requires the solution of the PDE at unconverged (and therefore non-aligned) meshes.

IV. Applications

A. One-dimensional inviscid Burgers' equation with discontinuous source term

The proposed high-order shock tracking framework is applied to the one-dimensional Burgers' equation with a discontinuous source term

$$\frac{\partial}{\partial x}\left(\frac{1}{2}u^2\right) = \beta u + f(x), \quad \text{for } x \in \Omega \subset \mathbb{R}, \tag{13}$$

where $\beta = -0.1$ and

$$f(x) = \begin{cases} (2 + \sin(\frac{\pi x}{2}))(\frac{\pi}{2}\cos(\frac{\pi x}{2}) - \beta), & x < 0 \\ (2 + \sin(\frac{\pi x}{2}))(\frac{\pi}{2}\cos(\frac{\pi x}{2}) + \beta), & x > 0. \end{cases} \tag{14}$$

It can be shown that the solution of (13) is

$$u(x) = \begin{cases} 2 + \sin(\frac{\pi x}{2}), & x < 0 \\ -2 - \sin(\frac{\pi x}{2}), & x > 0. \end{cases} \tag{15}$$

The domain is taken as $\Omega = (-2,\, 2)$ with Dirichlet boundary conditions specified at both ends corresponding to the exact solution, i.e., $u(-2) = 2$ and $u(2) = -2$. The discretization of (13) proceeds according to the formulation in Section II and the numerical flux is taken as the solution of the exact Riemann problem corresponding to the time-dependent version of (13) without source terms ($\beta = 0$ and $f(x) = 0$).

The proposed discontinuity-tracking framework is applied to solve Burgers' equation using very few high-order elements. The full space optimization approach discussed in Section III.D is used with SNOPT [14] as the nonlinear optimizer. The exact solution and initial guess for the solution, $\boldsymbol{u}$, and positions of the mesh nodes, $\boldsymbol{x}$, are shown in Figure 2. The initial mesh does not align with a shock, which causes the standard DG solution (used as the initial guess for $\boldsymbol{u}$) to oscillate. The solution of the shock tracking framework using 11 quadratic elements is shown in Figure 3 for several values of the upper bound on the mesh distortion, $\bar{f}_{msh}$. For large values of $\bar{f}_{msh}$, the mesh successfully tracks the shock, as expected; however, the mesh becomes distorted as f_{shk} favors large elements around regions where the solution has a zero (or nearly zero) slope. As the value of $\bar{f}_{msh}$ decreases, the quality of the mesh improves while still tracking the shock. Eventually, the mesh quality constraint becomes too restrictive and the mesh cannot simultaneously satisfy the element distortion constraints and track the shock. In this case, the optimizer returns a high-quality mesh (required by the distortion constraints) that does not track the shock.

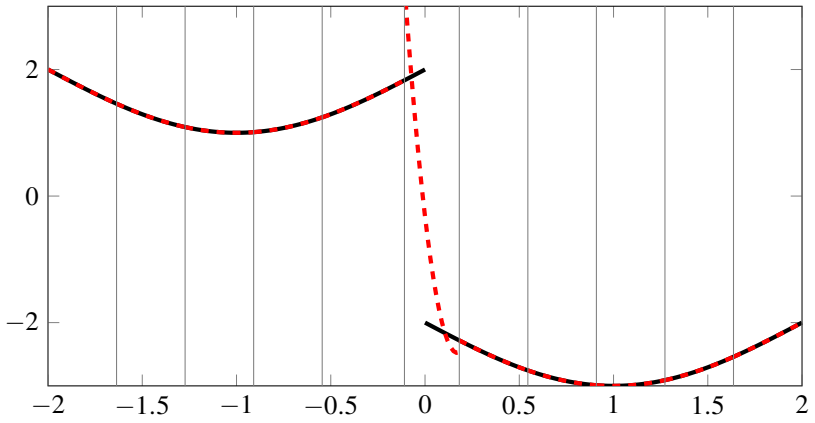

Fig. 2 The exact solution (——) to the inviscid Burgers' equation in (13) and the corresponding initial guess for the mesh (——) and solution (- - -) for the discontinuity-tracking framework on a discontinuous Galerkin discretization with 11 quadratic elements.

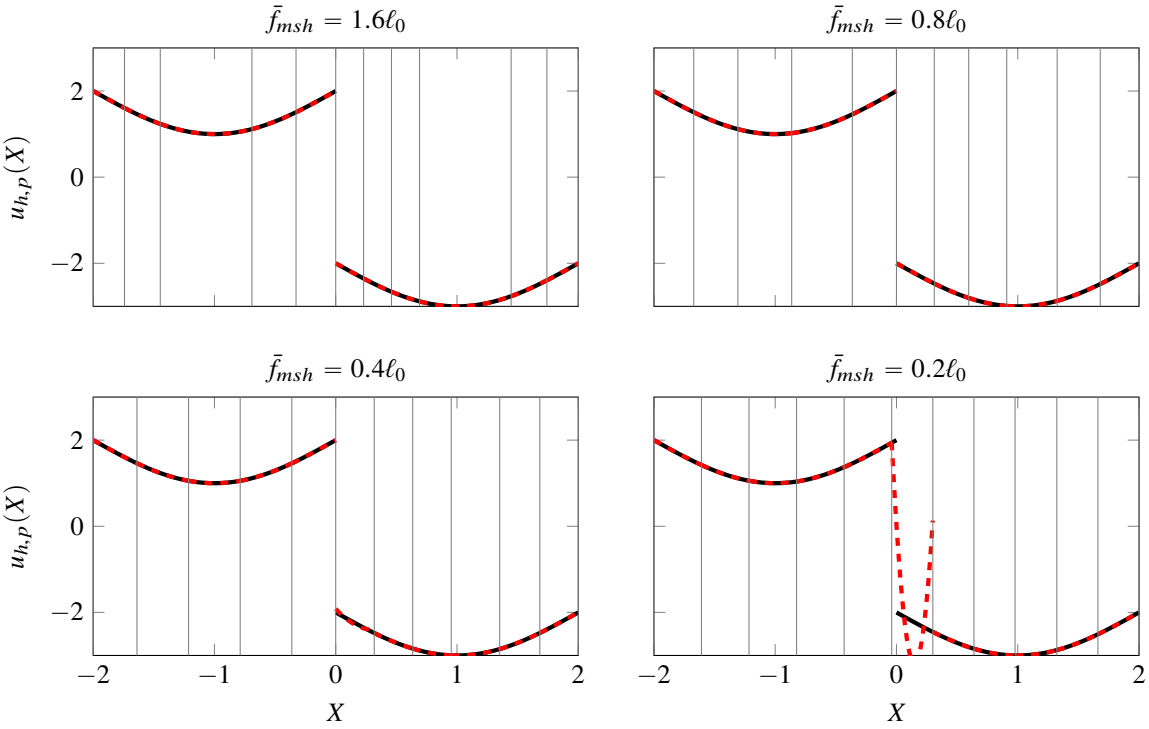

Fig. 3 Results of discontinuity-tracking framework applied to the solution of the inviscid Burgers' equation on a discretizations with 11 quadratic elements for a range of upper bounds on the mesh distortion: $\bar{f}_{msh} = 1.6\ell_0$ (top left), $0.8\ell_0$ (top right), $0.4\ell_0$ (bottom left), and $0.2\ell_0$ (bottom right), where $\ell_0 = |\Omega|/|\mathcal{E}_{h,p}| = 0.3636$ is the size of the uniform element. Legend: exact solution (——) of the inviscid Burgers' equation, mesh (——), and solution (- - -) obtained from discontinuity-tracking framework. As the value of $\bar{f}_{msh}$ decreases, the quality of the tracking mesh improves until $\bar{f}_{msh} = 0.2$ where the mesh distortion constraint is too restrictive that the mesh cannot sufficiently deform to track the shock.

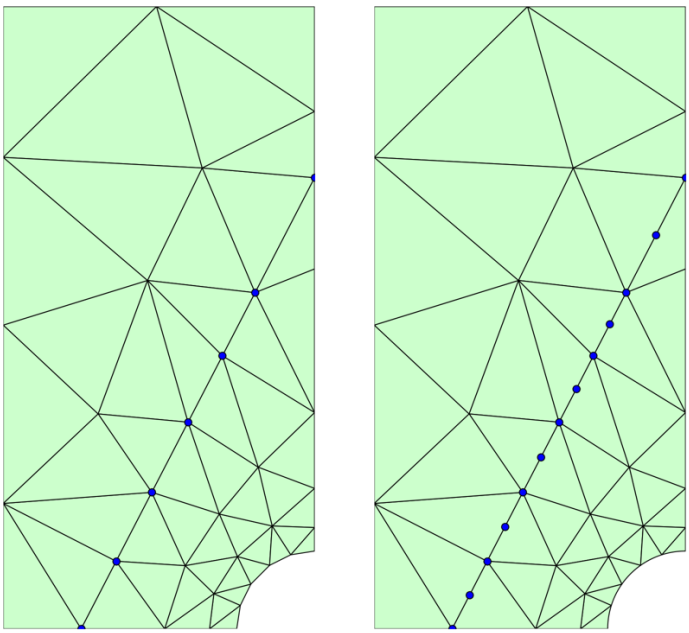

Fig. 4 Reference domain and mesh with $|\mathcal{E}_{h,p}| = 48$ elements and polynomial orders $p = 1$ (*left*) and $p = 2$ (*right*). The blue circles identify parametrized nodes, i.e., nodal positions that whose displacements compose the optimization variables $\boldsymbol{\phi}$. Only the displacement normal to the boundary are taken as optimization variables for the two parametrized nodes that lie on boundaries.

B. Supersonic flow around two-dimensional bluff body

In this section, we study the performance of the proposed discontinuity tracking framework on two-dimensional inviscid, supersonic flow around a circle. The geometry of the domain and reference mesh with $|\mathcal{E}_{h,p}| = 48$ elements are shown in Figures 4 for polynomial orders $p = 1$ and $p = 2$. The flow is modeled by the two-dimensional steady Euler equations

$$\begin{aligned} \frac{\partial}{\partial x_i}(\rho u_i) &= 0, \\ \frac{\partial}{\partial x_i}(\rho u_i u_j + p) &= 0 \quad \text{for } i = 1, 2, \\ \frac{\partial}{\partial x_i}\left(u_j(\rho E + p)\right) &= 0, \end{aligned} \tag{16}$$

where ρ is the fluid density, u_1, u_2 are the velocity components, and E is the total energy. For an ideal gas, the pressure p has the form

$$p = (\gamma - 1)\rho\left(E - \frac{1}{2}u_k u_k\right), \tag{17}$$

where γ is the adiabatic gas constant. The discretization of the governing equations proceed according to the formulation in Section II and Roe's approximate Riemann solver corresponding to the time-dependent version of (16) is used for the numerical flux. All farfield and inviscid wall boundary conditions are weakly imposed using the Roe solver. The incoming flow is taken as supersonic at Mach 2.

For simplicity, we use a simple mesh parametrization that does not include the position of all the nodes of the continuous high-order mesh, but rather a well-chosen subset of these nodes. The remainder of the nodes are determined through a linear operator that incorporates mesh smoothing. In this work, we use linear elasticity with prescribed displacements at the parametrized nodes and in the normal direction along domain boundaries. The free degrees of are shown in Figure 4 and lead to $N_{\boldsymbol{\phi}} = 12$ for $p = 1$ and $N_{\boldsymbol{\phi}} = 24$ for $p = 2$.

As a non-convex optimization problem underlies the discontinuity-tracking framework, the performance of the full space solver relies on a quality initial guess. Similar to [10], we use homotopy in p to initialize the discontinuity-tracking problems for polynomial orders beyond 1. That is, the discontinuity-tracking solution at polynomial order p is used to

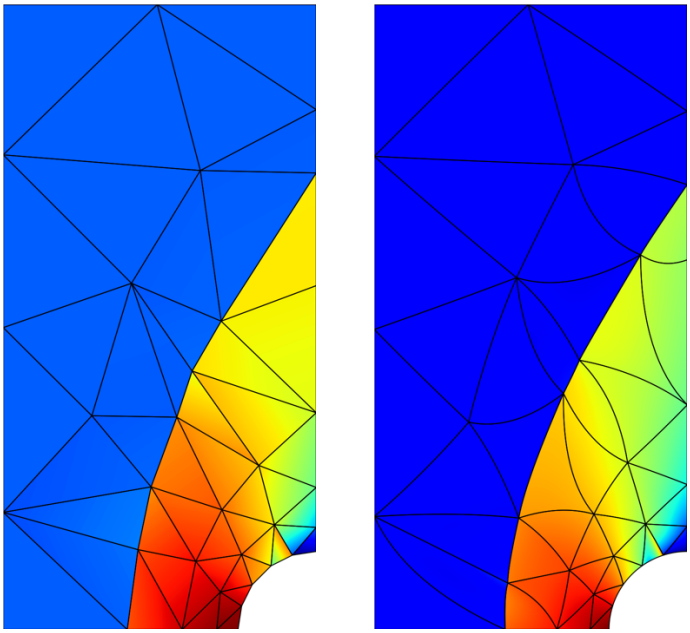

Fig. 5 Solution of two-dimensional Euler equations (density) with supersonic inflow $M = 2$ using discontinuity-tracking framework with polynomial orders $p = 1$ (*left*) and $p = 2$ (*right*). Both use a mesh distortion upper bound of $\bar{f}_{msh} = 0.12$. The deformed mesh provided by the tracking framework is included to show that high-quality curved elements track the shock location.

initialize the solver at polynomial order $p + 1$. This requires a simple injection operation to transfer the solution $\boldsymbol{u}$ and mesh $\boldsymbol{x}(\boldsymbol{\phi})$ to a higher polynomial degree.

The result of the discontinuity-tracking method using the above initialization strategy and the reference domain in Figure 4 is provided in Figure 5. For all polynomial orders, the shock is tracked as well as possible given the resolution limit of the mesh and the mesh distortion constraint, set to $\bar{f}_{msh} = 0.12$ here. The solution for the $p = 1$ mesh is clearly underresolved and the shock surface is faceted since the elements cannot bend in the piecewise linear setting. The $p = 2$ mesh delivers an accurate, smooth solution away from the shock and tracks the smooth, curved shock surface very well.

V. Conclusion

This document presented a high-order accurate, nonlinearly stable discontinuity-tracking framework for solving conservation laws with discontinuous solution features. The method leverages the discontinuities between elements present in the finite-dimensional solution basis in the context of a discontinuous Galerkin discretization to track discontinuities in the underlying solution. Central to the tracking framework is a PDE-constrained optimization formulation of the discrete conservation law whose objective pushes the mesh to align with discontinuities and constraints ensure the discrete conservation law is satisfied. Additional constraints, often called "side constraints" in the PDE-constrained optimization community, on the distortion of the elements of the mesh are included to ensure a reasonably conditioned mesh is maintained while tracking discontinuities. The optimization problem is solved using a full space optimization solver whereby the PDE solution and mesh simultaneously converge to their optimal values, ensuring the discrete PDE solution is never required on non-aligned meshes. The merit of the method is established on a one- and two-dimensional test problem where accurate solutions were obtained on coarse meshes.

Acknowledgments

This work was supported in part by the Luis W. Alvarez Postdoctoral Fellowship (MZ) by the Director, Office of Science, Office of Advanced Scientific Computing Research, U.S. Department of Energy under Contract No. DE-AC02-05CH11231 (MZ, PP) and by the AFOSR Computational Mathematics program under grant number FA9550-15-1-0010 (MZ, PP).

References

[1] Cockburn, B., and Shu, C.-W., "Runge-Kutta discontinuous Galerkin methods for convection-dominated problems," *J. Sci. Comput.*, Vol. 16, No. 3, 2001, pp. 173–261.

[2] Hesthaven, J. S., and Warburton, T., *Nodal discontinuous Galerkin methods*, Texts in Applied Mathematics, Vol. 54, Springer, New York, 2008. Algorithms, analysis, and applications.

[3] Peraire, J., and Persson, P.-O., *Adaptive High-Order Methods in Computational Fluid Dynamics*, World Scientific Publishing Co., 2011, Advances in CFD, Vol. 2, Chaps. 5 – High-Order Discontinuous Galerkin Methods for CFD.

[4] Baumann, C. E., and Oden, J. T., "A discontinuous *hp* finite element method for the Euler and Navier-Stokes equations," *Int. J. Numer. Methods Fluids*, Vol. 31, No. 1, 1999, pp. 79–95. Tenth International Conference on Finite Elements in Fluids (Tucson, AZ, 1998).

[5] Burbeau, A., Sagaut, P., and Bruneau, C.-H., "A problem-independent limiter for high-order Runge-Kutta discontinuous Galerkin methods," *J. Comput. Phys.*, Vol. 169, No. 1, 2001, pp. 111–150.

[6] Shu, C.-W., and Osher, S., "Efficient implementation of essentially nonoscillatory shock-capturing schemes," *J. Comput. Phys.*, Vol. 77, No. 2, 1988, pp. 439–471.

[7] Persson, P.-O., and Peraire, J., "Sub-Cell Shock Capturing for Discontinuous Galerkin Methods," *44th AIAA Aerospace Sciences Meeting and Exhibit, Reno, Nevada*, 2006. AIAA-2006-0112.

[8] Persson, P.-O., "Shock Capturing for High-Order Discontinuous Galerkin Simulation of Transient Flow Problems," *21st AIAA Computational Fluid Dynamics Conference, San Diego, CA*, 2013. AIAA-2013-3061.

[9] Von Neumann, J., and Richtmyer, R. D., "A method for the numerical calculation of hydrodynamic shocks," *J. Appl. Phys.*, Vol. 21, 1950, pp. 232–237.

[10] Zahr, M. J., and Persson, P.-O., "An optimization-based approach for high-order accurate discretization of conservation laws with discontinuous solutions," *Journal of Computational Physics*, Vol. 365, 2018, pp. 105 – 134. doi:https://doi.org/10.1016/j.jcp.2018.03.029, URL `http://www.sciencedirect.com/science/article/pii/S002199911830189X`.

[11] Persson, P.-O., Bonet, J., and Peraire, J., "Discontinuous Galerkin solution of the Navier–Stokes equations on deformable domains," *Computer Methods in Applied Mechanics and Engineering*, Vol. 198, No. 17, 2009, pp. 1585–1595.

[12] Knupp, P. M., "Algebraic Mesh Quality Metrics," *SIAM Journal on Scientific Computing*, Vol. 23, No. 1, 2001, pp. 193–218. doi:10.1137/S1064827500371499.

[13] Gargallo-Peiró, A., Roca, X., Peraire, J., and Sarrate, J., "A distortion measure to validate and generate curved high-order meshes on CAD surfaces with independence of parameterization," *International Journal for Numerical Methods in Engineering*, Vol. 106, No. 13, 2016, pp. 1100–1130. URL `https://doi.org/10.1002/nme.5162`.

[14] Gill, P. E., Murray, W., and Saunders, M. A., "SNOPT: An SQP algorithm for large-scale constrained optimization," *SIAM Journal on Optimization*, Vol. 12, No. 4, 2002, pp. 979–1006.